

Nitriding of titanium in electron beam excited plasma in medium vacuum



A.V. Tyunkov, D.A. Golosov, D.B. Zolotukhin, A.V. Nikonenko, E.M. Oks, Yu.G. Yushkov, E.V. Yakovlev

PII: S0257-8972(19)31231-9

DOI: <https://doi.org/10.1016/j.surfcoat.2019.125241>

Reference: SCT 125241

To appear in: *Surface & Coatings Technology*

Received date: 11 October 2019

Revised date: 5 December 2019

Accepted date: 6 December 2019

Please cite this article as: A.V. Tyunkov, D.A. Golosov, D.B. Zolotukhin, et al., Nitriding of titanium in electron beam excited plasma in medium vacuum, *Surface & Coatings Technology* (2019), <https://doi.org/10.1016/j.surfcoat.2019.125241>

This is a PDF file of an article that has undergone enhancements after acceptance, such as the addition of a cover page and metadata, and formatting for readability, but it is not yet the definitive version of record. This version will undergo additional copyediting, typesetting and review before it is published in its final form, but we are providing this version to give early visibility of the article. Please note that, during the production process, errors may be discovered which could affect the content, and all legal disclaimers that apply to the journal pertain.

# Nitriding of Titanium in Electron Beam Excited Plasma in Medium Vacuum

<sup>1,3</sup>Tyunkov A.V., <sup>2</sup>Golosov D.A., <sup>1</sup>Zolotukhin D.B., <sup>1</sup>Nikonenko A.V., <sup>1,3</sup>Oks E.M.,  
<sup>1,3</sup>Yushkov Yu.G., <sup>3</sup>Yakovlev E.V.

<sup>1</sup>Tomsk State University of Control Systems and Radioelectronics, 40 Lenin Avenue, Tomsk 634050, Russia

<sup>2</sup>Belarusian State University of Informatics and Radioelectronics, 6 P. Brovki Str., Minsk 220013, Belarus

<sup>3</sup>Institute of High Current Electronics SB RAS, 2/3 Akademichesky Ave., Tomsk 634055, Russia

*We report our results on nitriding of industrially-pure titanium VT1-0 in the plasma formed by continuous electron beam created by a fore-vacuum plasma-cathode electron source, at different temperatures of the titanium sample surface (700-1020 °C) and electron beam energy (4-6 keV), in medium vacuum (5 Pa) of nitrogen. Electron beam was used for direct treatment and heating of the sample as well as for the plasma generation. It is demonstrated that such parameters of the Ti sample as nitrogen content, the depth of nitride layer, Vickers microhardness, and wear-resistance grow with sample temperature and beam energy. Such positive effects happen, likely, due to enhanced generation of active atoms and atomic ions of nitrogen in beam-produced plasmas in medium vacuum.*

Keywords: plasma nitriding, fore-vacuum electron sources, titanium.

## INTRODUCTION

Titanium is among the top ten most abundant elements on Earth [1]. Titanium and its alloys in terms of their physical and mechanical properties are superior to steel and aluminum, the most widely used engineering materials of today. Titanium-based materials are characterized by high melting temperatures and hardness, on par with most brands of alloy steel; corrosion resistance in the air, water and chemically aggressive media; magnetization and other useful properties [1–2]. In addition, titanium is very light, its specific weight is 56% of that of steel, biologically inert [3] and yields easily to processing by pressure. As of today, titanium and its alloys with various properties are used as key materials in such strategic areas as aircraft and spaceship building [4], nuclear energy [5], ship building [6], medicine [7], food and chemical industries [8], and electronics [9]. The gamut of industries where titanium and its alloys find applications is actively expanding, which will allow advanced and highly efficient new-generation devices to be created in the nearest future.

The main constraining factors that stand in the way of wider application of titanium and its alloys in engineering are their low wear resistance and surface hardness, high accretion (viscosity) and a large value of the coefficient of friction in pair with most materials [1]. Among the efficient methods that improve the functional properties of titanium alloys are ion-plasma surface treatment [10], deposition of hardening coatings [10, 11], creation of modified surface layers by chemical-thermal treatment in nitrogen atmosphere [12-18], and ion implantation [19-21]. Much interest has been recently drawn to hardening of titanium alloys by modification of the surface layers by diffusion saturation with nitrogen. An obvious advantage of this method over depositing hardening coatings is the absence of adhesion. Unlike the ion implantation method, where the modified layer depth is several micrometers [19-21], diffusion saturation with nitrogen enables one to form layers up to hundreds of micrometers thick [12-18, 22] depending on the experimental parameters, the alloy chemical composition [22] and alloy additives [1, 2].

A number of techniques used to harden the surface of titanium and its alloys with nitrogen are grouped under the diffusion saturation method: gas nitriding [12-14], liquid nitriding in saline solutions [24], and plasma nitriding [15-17]. Nitriding in saline solutions enables one to achieve a significant increase of the surface layer hardness in a matter of several hours. A significant disadvantage of this method is that it is highly toxic and thus hazardous not only to the operating personnel but to the environment as well. On the contrary, gas nitriding, which was one of the first of the diffusion saturation methods to appear, is a non-toxic process. It runs at

high temperatures with the exposition time lasting for tens of hours. Plasma nitriding favorably differs from the above methods in that that the technological process takes up less time, the environment is not polluted and the gas and energy consumption is low [25]. Such process features stimulate a wide use of plasma nitriding for improving operating properties of various brands of steel [26, 27] and titanium [16]. Plasma nitriding of steel and titanium can be efficiently implemented not only by using various forms of gas discharge [17, 28] but also by using low-energy electron beams [15, 29-31], the so-called method of electron beam excited plasma (EBEP).

The key factor responsible for a high rate of nitriding in the electron beam plasma is generation of atomic nitrogen (both ions and neutrals), whose coefficient of diffusion is greater than that of molecular nitrogen. Typical range of pressure for EBEP during the nitriding process is 0.1-1 Pa. It has been noted in [32] that as pressure increases in the interaction region between the electron beam and nitrided sample, recombination of nitrogen molecular ions with participation of low-energy plasma electrons prevail and it can result in an increase of atomic nitrogen. In fact, according to the results of mass-spectrum analysis [31], pressure significantly affects creation of atomic nitrogen in the electron beam plasma. An increase of pressure from 2 to 8 Pa results in a manifold increase of concentration of atomic nitrogen ions in the beam plasma near the treated sample. Considering the indicated facts, it looks promising to use electron sources with a plasma cathode [33] operating in the pressure range 2 – 20 Pa for nitriding various brands of steel and metals.

In this work, we present the results of nitriding of industrially pure titanium VT1-0 in the electron beam formed by a forevacuum plasma cathode electron source at different temperatures of the sample surface and electron beam energy.

## EXPERIMENT

The experimental setup for nitriding of titanium is shown in Fig. 1. The forevacuum hollow cathode plasma source of a continuous electron beam was mounted on the flange of the vacuum chamber. The electrode system and the working principle of the source are discussed in details in [31, 33].

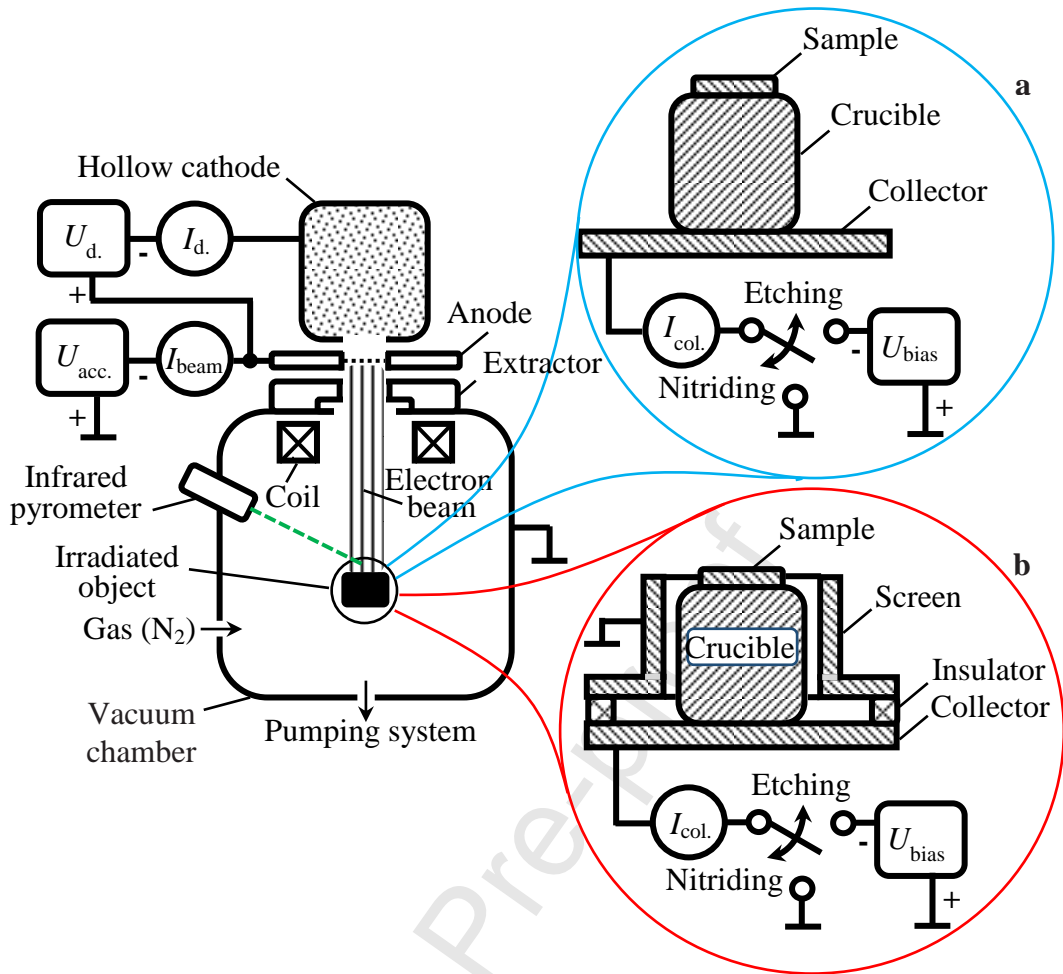


Figure 1 – Experimental setup: a – diagram of the irradiated sample for studying the temperature dependence; b – diagram of the irradiated sample for studying dependence on the electron energy (accelerating voltage).

The plasma electron source was fed by constant voltage sources connected to the discharge and accelerating gaps. The discharge voltage  $U_d = 360$  V, applied between the anode and the hollow cathode, ignited a glow discharge with discharge current  $I_d = 160$  mA. Electrons were extracted through a perforated tantalum plate in the anode. Upon applying the accelerating voltage, electron acceleration and primary formation of the beam took place in the anode-extractor gap. The electron beam was then focused by the magnetic field of a short coil, after which the beam was finally shaped. The beam plasma was generated in the electron beam transport region. The electron beam served as a heating source for the sample. The sample temperature was monitored by an optical pyrometer Raytek. The working chamber was pre-evacuated to a pressure of  $5 \cdot 10^{-3}$  Pa using a turbomolecular pump nEXT300D at a pump rate 300 l/s and then nitrogen (99.999%) was puffed into the chamber to the required working pressure. Plasma-cathode electron source was working in isobaric mode (i.e. without additional gas flow into hollow cathode of the source).

As previously mentioned, the presence of additives affects the properties of titanium alloys, so in order to minimize their influence on the structure and the phase state of the surface layers and the nitrogen diffusion rate, we used industrial titanium VT1-0, 3 mm thick with a diameter 20 mm, as a nitrided sample. The surface of the sample was polished by sandpaper and then cleaned with acetone and ethanol. Prior to nitriding, the sample surface was etched in argon (99.998 %) to remove the natural oxide film by applying a negative bias voltage of 250 V.

Additionally, the samples were preliminary subjected to heating by an electron beam in nitrogen. During the nitriding process, the treated sample was electrically grounded (Figs 1a and 1b). The heating and etching parameters are shown in Table 1.

Table 1 – Etching and preliminary heating parameters

| Etching         |       | Preliminary heating        |           |
|-----------------|-------|----------------------------|-----------|
| Parameter       | Value | Parameter                  | Value     |
| $U_{acc}$ , kV  | 3     | $U_{acc}$ , kV             | 3         |
| $U_{bias}$ , V  | 250   | $I_{beam}$ , mA            | 100       |
| $I_{beam}$ , mA | 100   | $I_{col}$ , mA             | a-45; b-5 |
| $I_{col}$ , mA  | 12    | $p$ , Pa                   | 5         |
| $p$ , Pa        | 2     | $time$ , min.              | 30        |
| $time$ , min.   | 20    | $t_{sample}$ , $^{\circ}C$ | 550       |

When studying the effect of the sample temperature on the properties of modified layer, the tantalum crucible with the sample was placed on the collector that was connected to an ammeter (Fig. 1b). The ammeter readings were used to set cross dimensions of the electron beam, and the beam diameter was comparable with that of the collector (9 cm). The sample temperature was increased by increasing the power of the beam electrons reaching the collector. The effect of accelerating voltage on the surface properties was studied at a constant electron beam power acting on the sample, thus maintaining a constant temperature of the sample. To provide this condition, the crucible with sample was put inside a screen, electrically grounded and isolated from the collector (Fig. 1b). An increase of the accelerating voltage was offset by decreasing the current on the sample via defocusing the electron beam. The experimental parameters are shown in Table 2.

Table 2 – Experimental parameters

| Effect of temperature      |     |     |     |      | Effect of electron beam energy<br>(accelerating voltage) |      |     |     |
|----------------------------|-----|-----|-----|------|--|------|-----|-----|
| Sample<br>Parameter        | #1  | #2  | #3  | #4   | Sample<br>Parameter                                      | #5   | #6  | #7  |
| $U_{acc}$ , kV             | 4   | 4,5 | 5   | 5,5  | $U_{acc}$ , kV   | 4    | 5   | 6   |
| $I_{beam}$ , mA            | 100 | 100 | 100 | 100  | $I_{beam}$ , mA  | 140  | 140 | 140 |
| $I_{col}$ , mA             | 45  | 45  | 45  | 45   | $I_{col}$ , mA   | 13.5 | 11  | 9   |
| $p$ , Pa                   | 5   | 5   | 5   | 5    | $p$ , Pa   | 5    | 5   | 5   |
| $time$ , min.              | 60  | 60  | 60  | 60   | $time$ , min.  | 60   | 60  | 60  |
| $t_{sample}$ , $^{\circ}C$ | 700 | 820 | 920 | 1020 | $t_{sample}$ , $^{\circ}C$                               | 820  | 820 | 820 |

The elemental composition of nitrated samples was analyzed using a Hitachi S3400N scanning electron microscope coupled with a BrukerX'Flash 5010 energy-dispersive detector. X-ray diffraction analysis (XRD) of the modified layer composition was conducted using a Shimadzu XRD-6000 X-ray diffractometer with a wavelength selected  $CuK\alpha$ -radiation in the direct-beam geometry. The phase composition was analyzed using the PDF 4+ database and the full-profile analysis software POWDER CELL 2.4. The XRD analysis is based on the phenomenon of X-ray diffraction on the crystalline lattice of the sample under study. With the help of the XRD method, we have determined the phase composition of the sample, dimensions of the coherent-scattering region (CSR), the lattice parameters and the lattice deformation ( $\Delta d/d$ ) of the formed layer.

The tribological characteristics at room temperature were measured by a Pin-on Disc and Oscillating TRIBO tribometer. This instrument uses the ball-on-disk measuring technique. The tested sample is rubbed against a ball tip with a 2 N load. The tip is fixed to a rigid lever which works as a frictionless force transducer. The tip was made of tungsten carbide. The coefficient of friction was determined during the test by measuring the deflection of the elastic lever. The material wear was determined by measuring the wear track created during the test. The wear

parameter, indicative of the rate of wear, was determined by the formula  $V=2\pi RA/FL$ , where R is the track radius,  $\mu\text{m}$ ; A is the cross-section area of the wear slot,  $\mu\text{m}^2$ ; F is the applied load, N; L is the distance traveled by the ball, m.

The surface hardness (H) was determined using the Vickers micro-hardness test. A diamond indenter with a square cross section and dihedral angle  $136^\circ$  acted on the sample surface at different points with the same load of 100 g. There were taken measurements of the indenter penetration depth and the indenture area. The nitrogen penetration depth, and consequently the modified layer thickness, was measured by preparing cross sections of the samples. The surface hardness of the sample cross sections was determined with the help of a Nanotest 600 nanoidentor by the Oliver-Pharr procedure using the Berkovich trigonal pyramid with the axis-facet angle  $65.03^\circ$ .

## EXPERIMENTAL RESULTS

### EFFECTS OF THE SURFACE TEMPERATURE ON NITRIDING

Analyses of the nitrided surfaces by SEM have shown that in the modified layers there are prevailing peaks of nitrogen, carbon, and titanium (Fig. 2, b); and only one sample nitrided at  $1020^\circ\text{C}$  contained a small amount of oxygen (4.4 wt. %). The small content of oxygen and carbon in the modified layer is related to their presence in the surface layer of titanium and, as shown in [34], such quantities do not degrade the nitrided layers. The intensity of carbon peaks was low (according to SEM studies), and therefore, after recalculating, this resulted in carbon percentage below the error level (see Fig. 2, c). However, a possible source of carbon in samples may be the contaminations from the environment outside the vacuum chamber.

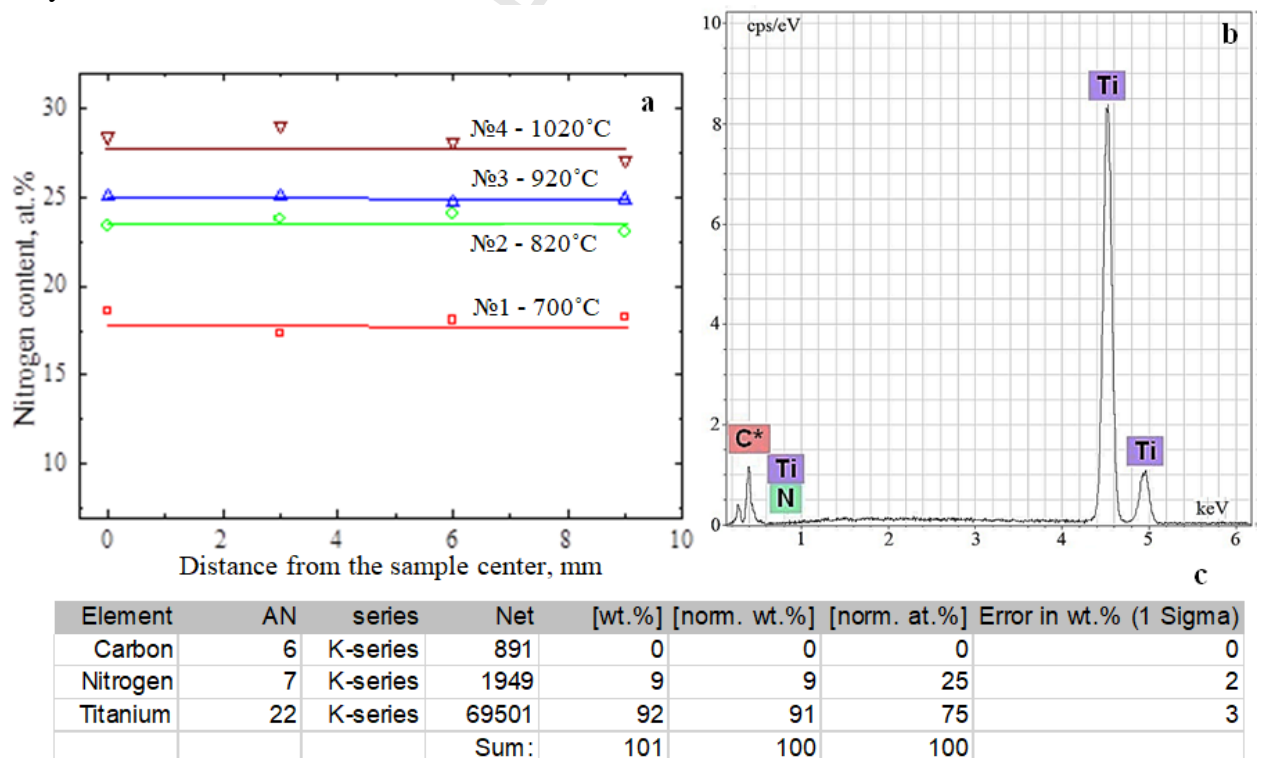


Figure 2 – Scanning electron microscopy of samples #1–#4: a – uniformity of nitrogen distribution in the surface layer vs. temperature; b – typical spectrum (the point at the edge of sample #3); c – quantitative elemental analysis at the edge of sample #3 (with 1 wt. % instrumental error).



It has been established that with increasing sample temperature the number of nitrogen atoms diffusing into the surface increases (Fig. 2a). Taking into account the well-known fact that during SEM study, the characteristic radiation from e-beam-irradiating materials comes from the depths of 1-2  $\mu\text{m}$ , it is reasonable to assume that at such depths nitride layers with different phase compositions are formed. It is a conspicuous fact that the quantities of nitrogen in sample 2 – 820  $^{\circ}\text{C}$  and sample 3 – 920  $^{\circ}\text{C}$  (Fig. 2a), nitrided at temperatures close to that of titanium  $\alpha$ - $\beta$  transformation, differ insignificantly. We believe this circumstance is related to formation of titanium nitride cubic lattice of NaCl-type on the surface of sample 3, which, as known [35], hampers the nitrogen diffusion into the sample surface layers. The absence of the edge effects caused by the ions due to non-uniformity of the electric field at the sample edges allows one to form the nitrogen layers distributed over the sample surface with non-uniformity not exceeding several percent. The assumed formation of the nitride layer with cubic lattice is confirmed by the results of X-ray analysis (Fig. 3 and Table 3).

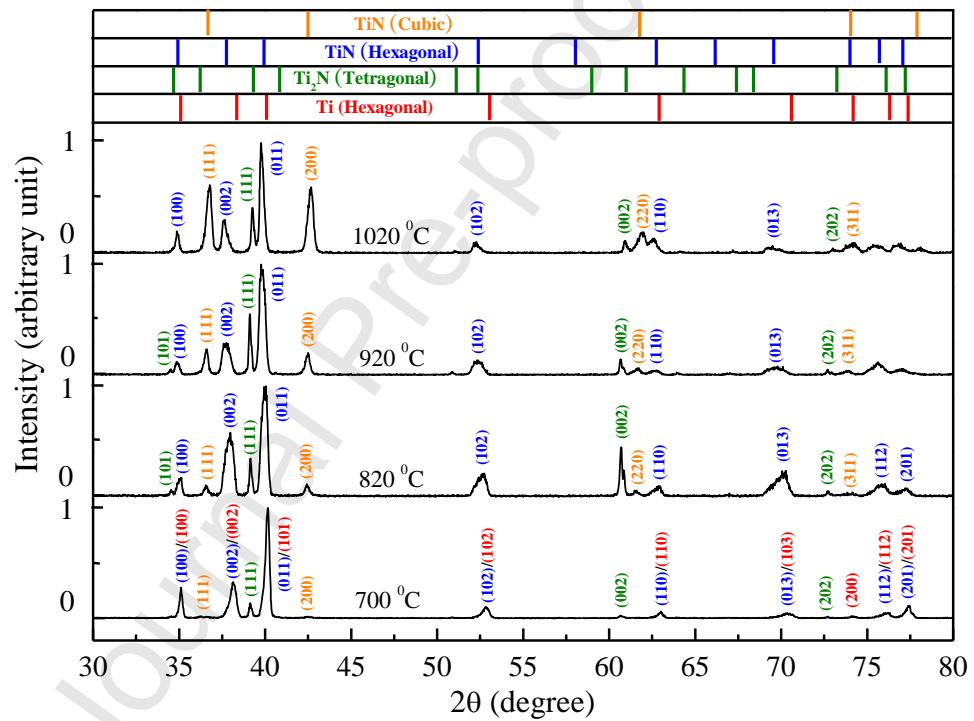


Figure 3 – X-ray analysis of the samples nitrided at different temperatures.

Table 3 - X-ray analysis of the samples nitrided at different temperatures.

| Sample                          | Phase                 | Phase content, mass % | Lattice parameters, $\text{\AA}$ | Size of CSR, nm | $\Delta d/d \cdot 10^{-3}$ |
|---------------------------------|-----------------------|-----------------------|----------------------------------|-----------------|----------------------------|
| #1<br>(700 $^{\circ}\text{C}$ ) | Ti_194                | 55                    | a = 2.9458<br>c = 4.7115         | >100            | 0.3                        |
|                                 | TiN_164               | 40                    | a = 2.9548<br>c = 4.7160         | 54              | 0.7                        |
|                                 | TiN_225               | <1                    | -                                | -               | -                          |
|                                 | Ti <sub>2</sub> N_136 | 5                     | a = 4.9471<br>c = 3.0501         | 36              | 1.7                        |
| #2<br>(820 $^{\circ}\text{C}$ ) | Ti_194                | -                     | -                                | -               | -                          |
|                                 | TiN_164               | 88                    | a = 2.9609<br>c = 4.7456         | 67              | 3.6                        |

|                 |                       |    |                          |      |     |
|-----------------|-----------------------|----|--------------------------|------|-----|
|                 | TiN_225               | 6  | a = 4.2599               | 69   | 0.6 |
|                 | Ti <sub>2</sub> N_136 | 6  | a = 4.9200<br>c = 3.0512 | 67   | 2.3 |
| #3<br>(920 °C)  | Ti_194                | -  | -                        | -    | -   |
|                 | TiN_164               | 72 | a = 2.9662<br>c = 4.7636 | 32   | 0.8 |
|                 | TiN_225               | 16 | a = 4.2516               | 47   | 0.9 |
|                 | Ti <sub>2</sub> N_136 | 12 | a = 4.9720<br>c = 3.0436 | 56   | 0.5 |
| #4<br>(1020 °C) | Ti_194                | -  | -                        | -    | -   |
|                 | TiN_164               | 42 | a = 2.9667<br>c = 4.7781 | 57   | 0.7 |
|                 | TiN_225               | 48 | a = 4.2348               | 33   | 1.2 |
|                 | Ti <sub>2</sub> N_136 | 10 | a = 4.9396<br>c = 3.0384 | >100 | 0.3 |

Table 3 shows that the lattice parameters for the TiN<sub>164</sub> phase increase with the nitriding temperature, but for the TiN<sub>225</sub> phase they decrease. Changes in the lattice parameters may indicate the formation of internal micro-stresses or structural defects. It should be expected that the formed layers have a nano-scale structure, as evidenced by the characteristic values of coherent scattering regions.

As seen, the titanium nitride phase with cubic lattice (TiN) increases with increasing temperature and becomes dominant at temperatures above 820 °C. Apart from the phase with cubic lattice, the samples also contain the titanium nitride phases with hexagonal (TiN<sub>0.26</sub>) and tetragonal (Ti<sub>2</sub>N) lattices. Since for the direct-beam mode, the layer depth from which the X-ray readings can be received may reach tens of μm, the absence of α-titanium at temperatures above 700 °C signifies an extended dimension of the nitrated (diffused) layer with increasing temperature. The presence of weak reflexes, corresponding to hexagonal and tetragonal titanium nitride, as well as the presence of α-titanium peaks, indicates at a relatively small thickness of the diffused layer in the sample nitrated at 700 °C. This fact may testify to low performance properties (wear resistance and hardness). It is mostly due to a relatively short period of nitriding, therefore it is necessary to increase the process duration in order to improve the sample performance properties.

The increase of the sample surface hardness with increasing temperature (Fig. 4) is related to both an increased concentration of nitrogen in the surface layer and formation there of nitride titanium phases with cubic and tetragonal lattices. Thereby the surface hardness increases by 3-6 times as temperature grows.



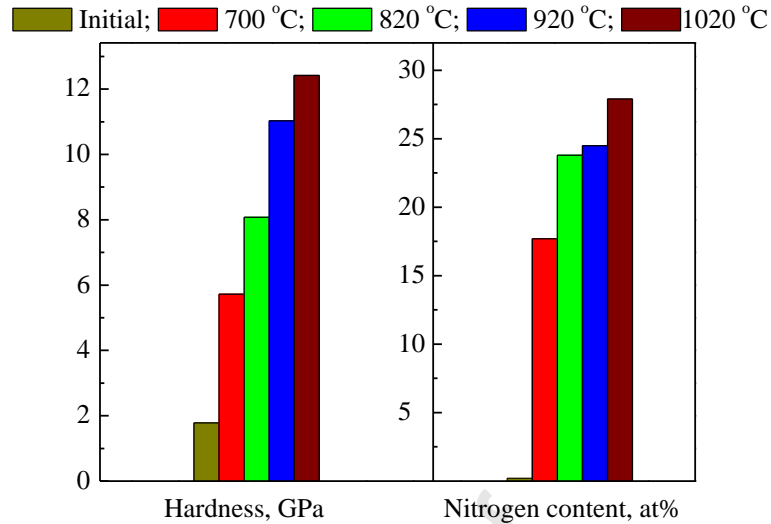


Figure 4 – Surface hardness and concentration of nitrogen in the surface layer versus temperature.

The maximal value of the surface hardness is less than the hardness of stoichiometric titanium nitride. We believe this is due to a relatively small thickness of the formed TiN layer. Such assumption is corroborated by the X-ray analysis which registers, apart from cubic titanium nitride with a 48% content, other titanium nitride phases. It should be noted that an hour-long nitriding suffices to significantly increase the surface hardness even at low-temperature nitriding.

Despite small contents of nitride phases in sample #1, nitriding at 700 °C results in a manifold (from  $122 \cdot 10^{-5} \text{ mm}^3/\text{Nm}$  to  $4.9 \cdot 10^{-5} \text{ mm}^3/\text{Nm}$ ) decrease of the surface wear rate (Fig. 5). Increasing the nitriding temperature to 820 °C improves the wear resistance by an order of magnitude to  $0.4 \cdot 10^{-5} \text{ mm}^3/\text{Nm}$ . Further temperature increase does not affect the sample surface wear rate.

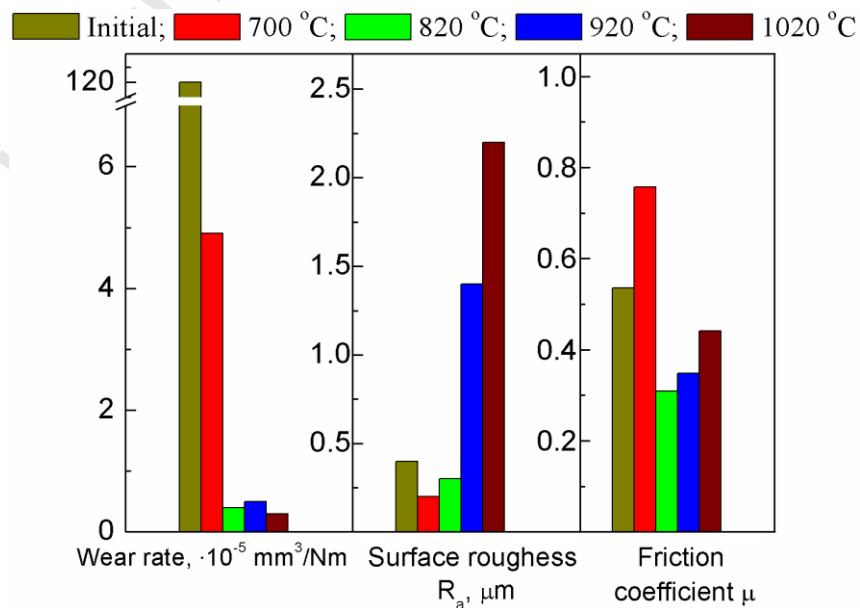


Figure 5 – Results of tribological tests.

It should be noted that the surface roughness  $R_a$  both of the samples nitrided at temperatures below polymorphic transition and that of the original sample lie within 0.2-0.4  $\mu\text{m}$ . The difference for each sample is due to its surface preparation. However, nitriding at

temperatures above the temperature of polymorphic transition sharply increases the surface roughness, up to 2.2  $\mu\text{m}$ . The data on the sample surface roughness comply with the SEM images (Fig. 6). In contrast to the surface of sample #1 – 700°C, the surface of sample #4 – 1020°C looks strongly melted, which is the cause of an increase of the parameter  $R_a$ .

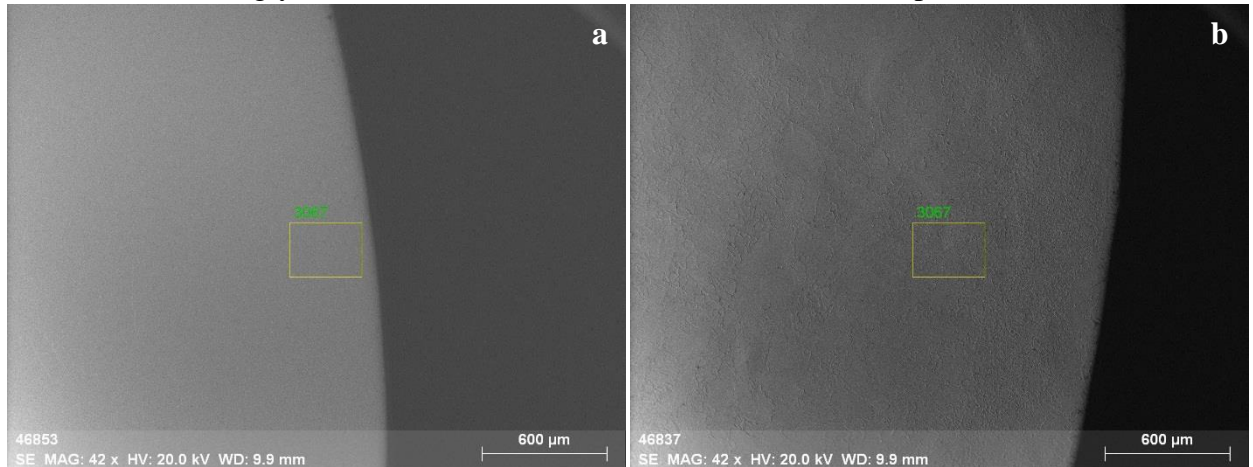


Figure 6 – SEM images of nitrided samples: a – sample #1 (700°C); b – sample #4 (1020°C)

The high value of the coefficient of friction  $\mu$  of the sample can be attributed to a low content of nitride phases in the modified layer and its small space extension at the nitriding temperature 700°C. Increasing the nitriding temperature to 820°C noticeably decreases the coefficient of friction from 0.53 to 0.3. On further increasing the nitriding temperature, the coefficient of friction begins to increase, which can be connected with a significant increase of the surface roughness.

The nitrogen penetration depth into the sample also increases with increasing temperature (Fig. 7).

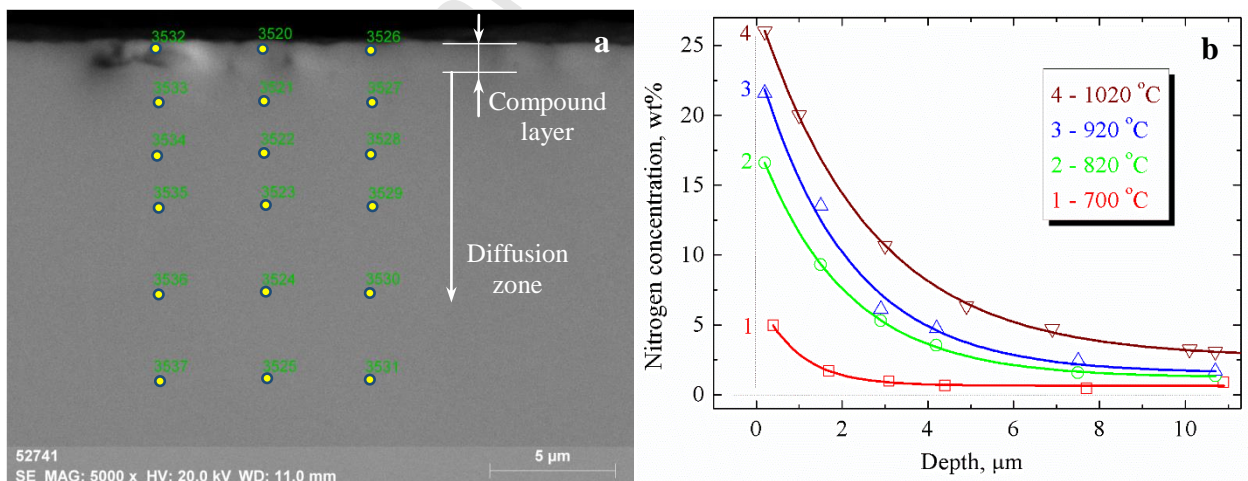


Figure 7 – Concentration of nitrogen vs. the sample depth: a) – a SEM cross section image; b) – the nitrogen distribution.

It has been established that with increasing temperature the nitrogen concentration increases both at the plane of the sample surface and with depth. There is also observed a growth of the «compound layer» (the layer containing TiN and  $\text{Ti}_2\text{N}$ ) from 0.5 to 2  $\mu\text{m}$  with increasing temperature. The SEM data are supported by measurements of the hardness versus the sample depth (Fig. 8).

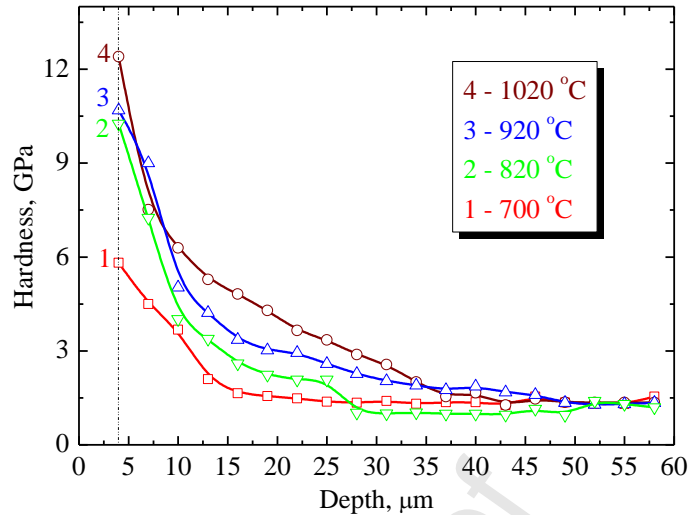


Figure 8 – Hardness vs. depth for different nitriding temperatures. Each data point was obtained after averaging over five measuring trials.

The thickness of the modified (diffusion) layer, determinable by the nitrogen concentration, and, therefore, hardness increase with increasing nitriding temperature up to the depths  $\sim 15 \mu\text{m}$  at  $700^\circ\text{C}$  and  $\sim 35\text{--}45 \mu\text{m}$  at  $920\text{--}1020^\circ\text{C}$  (Fig. 8). Note that the hardness measurements of the cross section surfaces were carried out starting from the point  $4 \mu\text{m}$  off the edge of the sample due to specifics of the employed measurement technique. Considering the length of the «compound layer», one should expect higher values of hardness in the range  $0.1 - 4 \mu\text{m}$ .

To sum up, increasing of the nitriding temperature in the electron beam plasma in medium vacuum increases, as is the case for the discharge plasma, the nitrogen concentration in the surface layer, extended “compound layer” and diffusion zone, which effects the hardness of surface and deeper layers, and wear resistance. It is all related to the nitrogen diffusion capacity to penetrate into the sample surface layers at a given temperature. However, the nitriding time in the electron beam plasma required to attain the surface layer parameters, comparable with those obtainable in discharge plasma and other nitrogen diffusion saturation methods, is significantly less, which we believe is due to generation of a large quantity of atomic nitrogen, in the form of ions and neutrals, in medium vacuum (in the working pressure range of forevacuum electron sources).

#### EFFECTS OF ELECTRON BEAM ENERGY

Fig. 9 and Table 4 show the results of X-ray analysis of the samples nitrided at different energies of the electron beam.

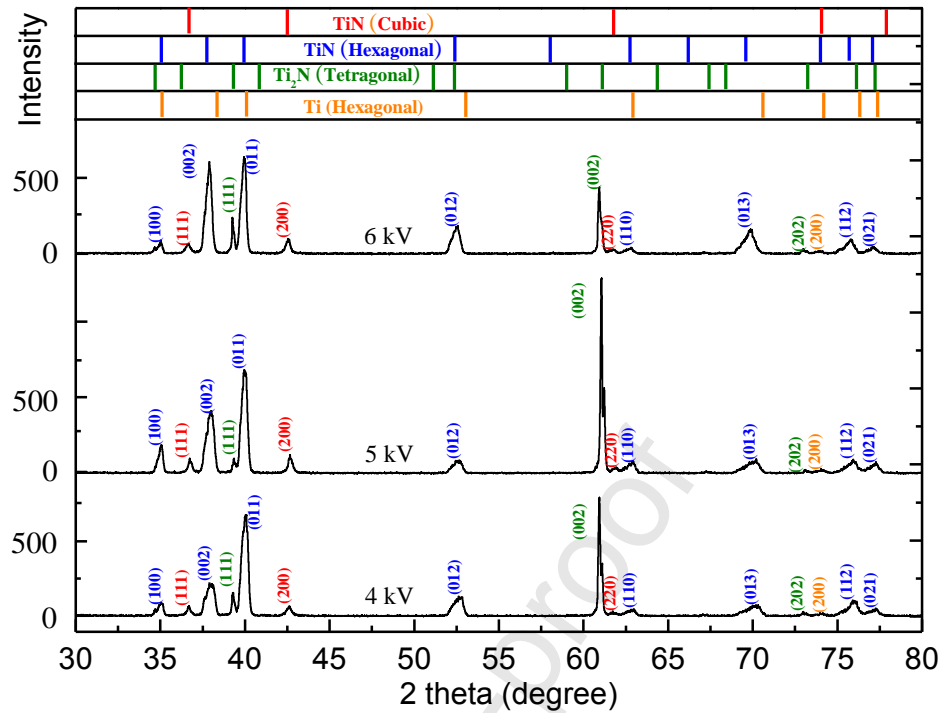


Figure 9 – X-ray analysis of the samples nitrided at different energies of the electron beam.

Table 4 – X-ray analysis of the samples nitrided at different energies of the electron beam

| Sample        | Phase                 | Phase content mass % | Lattice parameters, Å    | Size of CSR, nm | $\Delta d/d \cdot 10^{-3}$ |
|---------------|-----------------------|----------------------|--------------------------|-----------------|----------------------------|
| #5<br>(4 keV) | Ti_194                | <1                   | -                        | -               | -                          |
|               | TiN_164               | 82                   | a = 2.9582<br>c = 4.7469 | 37              | 2.3                        |
|               | TiN_225               | 6                    | a = 4.2443               | 53              | 0.8                        |
|               | Ti <sub>2</sub> N_136 | 12                   | a = 4.9401<br>c = 3.0399 | >100            | 1.0                        |
| #6<br>(5 keV) | Ti_194                | 3                    | a = 2.9561<br>c = 4.7136 | 32              | 4.0                        |
|               | TiN_164               | 89                   | a = 2.9570<br>c = 4.7508 | 54              | 3.2                        |
|               | TiN_225               | 8                    | a = 4.2348               | 73              | 0.6                        |
|               | Ti <sub>2</sub> N_136 | 9                    | a = 4.9379<br>c = 3.0334 | >100            | 0.3                        |
| #7<br>(6 keV) | Ti_194                | <1                   | -                        | -               | -                          |
|               | TiN_164               | 82                   | a = 2.9579<br>c = 4.7482 | 44              | 3.3                        |
|               | TiN_225               | 8                    | a = 4.2458               | 39              | 1.0                        |
|               | Ti <sub>2</sub> N_136 | 10                   | a = 4.9392<br>c = 3.0380 | >100            | 0.3                        |

Table 4 shows that the layers formed have a nanoscale structure, and the corresponding phases of titanium nitride have similar lattice parameters regardless of the electron energy at which the layers are formed. It has been established that the samples predominantly contain titanium nitride with a hexagonal lattice. Small contents of tetragonal and cubic phases of titanium nitride may speak for a small extension of the «compound layer». Increasing the

electron beam energy does not materially affects the sample structure or phase composition. However, with increasing beam energy, the nitrogen concentration in the surface layer and the surface hardness increase (Fig. 10) We have not revealed any significant differences in the values of wear resistance, roughness, or friction related to the beam energy used in nitriding. Nevertheless, all nitrided samples exhibited a significant decrease of the wear rate and the coefficient of friction as compared to the original samples.

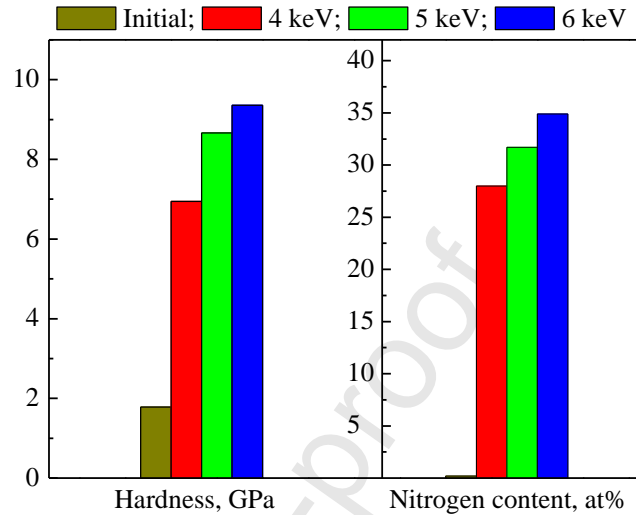


Figure 10–Dependence of the surface hardness and nitrogen content on the electron beam energy

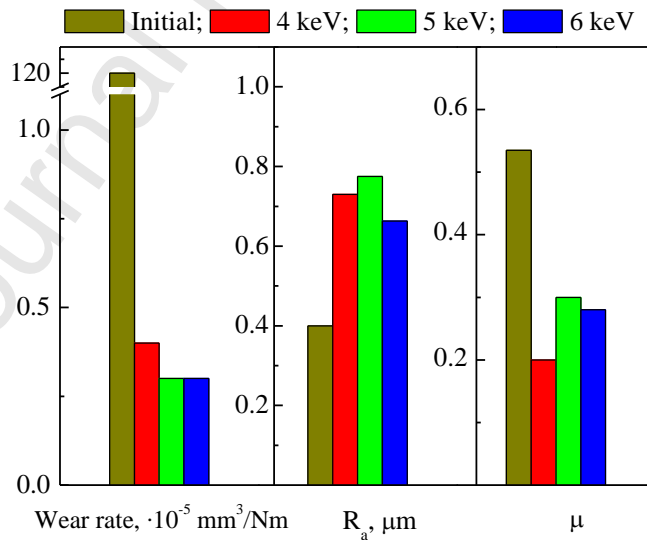


Figure 11 – Tribological tests of the samples nitrided at different electron beam energies

With increasing electron energy, the nitrogen penetration depth and, therefore, the thickness of modified (diffusion) layer and hardness increase up to depths 40  $\mu\text{m}$  at 4 keV and 60  $\mu\text{m}$  at 6 keV (Fig. 12), while the length of the «compound layer» is about 1  $\mu\text{m}$  for all three samples.

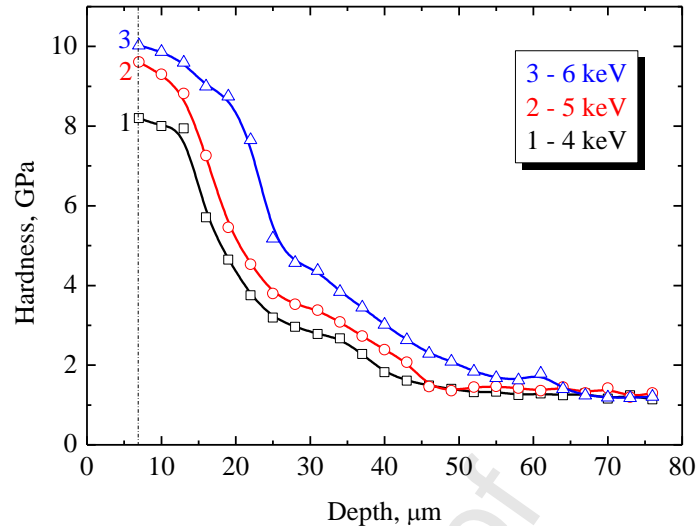


Figure 12 – Hardness profile for different electron beam energies.

It should be noted that the active factor that affects the surface properties of a nitrided sample, as the beam energy increases from 4 to 6 keV, is generation of a large quantity of atomic nitrogen ions and neutrals [31].

## CONCLUSION

The experimental studies of nitriding of industrially pure titanium using a forevacuum plasma electron source have shown that the “compound layer” extension and the nitrogen concentration on the sample surface and with depth increase with increasing nitriding temperature. There is also observed an increase of titanium nitride phase with a cubic lattice, which results in a manifold increase of the surface hardness and significant decrease of the wear rate. An increase of the electron beam energy or current, under otherwise equal conditions, leads to an increased concentration of nitrogen in the surface layer, increased hardness and extension of the diffusion zone. However, the indicated changes of parameters do not affect the sample structure, phase composition, extension of the “compound layer” or tribological properties. It should be noted that despite the short duration of the nitriding process (1 hour), the attainable characteristics of modified layers are on par with those obtainable under usually employed nitrogen diffusion saturation methods that may last for several hours. It happens because of generation of a large number of atomic nitrogen ions and neutrals in the plasma excited by the electron beam operating in medium vacuum. The advantage of our method over the plasma-immersion ion implantation is the formation of nitride layers with a much higher thickness of tens of microns, thanks to the high diffusion of the atomic nitrogen due to direct sample heating with electron beam and relatively high nitrogen pressures (medium vacuum) used. In terms of the functional properties, the most efficient proves to be nitriding carried out at 820 °C. In spite of lower values of the surface hardness, as compared with that obtained at higher temperatures, the samples nitrided at 820 °C have a comparable wear rate but significantly less roughness, and, therefore, the lower coefficient of friction, which is important for friction pair parts. An optimal way of extending the diffusion zone, i.e. obtaining the surface hardness comparable with the samples nitrided at higher temperature, is to increase the electron beam energy.

## ACKNOWLEDGEMENT



The work was supported by the joint Russian – Belarusian research program grant #18-58-00004 (Russian Foundation for Basic Research) and the grant #T18P-092 (Belarusian Republican Foundation for Fundamental Research).

## REFERENCES

- [1] R. Boyer, G. Welsh, E.W. Collings, *Materials Properties Handbook-Titanium Alloys*, ASM International, Materials Park, OH, 1994.
- [2] E.W. Collings, *The Physical Metallurgy of Titanium Alloys*, American Society for Metals, 1984.
- [3] J. Emsley, *Nature's Building Blocks: An A-Z Guide to the Elements*, Oxford University Press, 2003
- [4] Eylon, D., Seagle, S.R. *Advances in titanium technology // Keikinzoku/Journal of Japan Institute of Light Metals*. Volume 50, Issue 8, 2000, Pages 359-370
- [5] S.J.Zinkle, G.S. Was *Materials challenges in nuclear energy // Acta Materialia*. Volume 61, Issue 3, February 2013, Pages 735-758
- [6] I.V. Gorynin, *Titanium alloys for marine application // Materials Science and Engineering: A* Volume 263, Issue 2, 1999, Pages 112-116
- [7] F. Galliano, E. Galvanetto, S. Mischler, D. Landolt. *Tribocorrosion behavior of plasma nitrided Ti-6Al-4V alloy in neutral NaCl solution // Surface and Coatings Technology*. 145 2001 121-131
- [8] M. S. Jellesen, A. A. Rasmussen, L. R. Hilbert *A review of metal release in the food industry // Materials and Corrosion*. 2006, 57, No. 5 387-392.
- [9] John Difonzo, Stephen Zadesky, David Lundgren *Use of titanium in a notebook computer US Patent 6,574,096 B1 Jun. 3, 2003*
- [10] Yongqing Fu, Nee Lam Loh, Andrew W. Batchelor, Daoxin Liu, Xiaodong Zhu, Jaiwen He, Kewei Xu *Improvement in fretting wear and fatigue resistance of Ti-6Al-4V by application of several surface treatments and coatings // Surface and Coatings Technology* 106 (1998) 193-197
- [11] J.A. Sue *Development of arc evaporation of non-stoichiometric titanium nitride coatings // Surface and Coatings Technology* 61 (1993) 115-120.
- [12] A. Zhecheva, S. Malinov, W. Sha, *Titanium alloys after surface gas nitriding // Surface & Coatings Technology* 201 (2006) 2467-2474.
- [13] Liling Ge, NaTian, Zhengxin Lu, Caiyin You. *Influence of the surface nanocrystallization on the gas nitriding of Ti-6Al-4V alloy // Applied Surface Science* Volume 286, 1 December 2013, Pages 412-416
- [14] Masaaki Nakai, Mitsuo Niinomi, Toshikazu Akahori, Naofumi Ohtsu, Hideki Nishimura, Hiroyuki Toda, Hisao Fukui, Michiharu Ogawa. *Surface hardening of biomedical Ti-29Nb-13Ta-4.6Zr and Ti-6Al-4V ELI by gas nitriding // Materials Science and Engineering: A* Volume 486, Issues 1-2, 15 July 2008, Pages 193-201
- [15] Gavrilov, N.V., Mamaev, A.S. *Low-temperature nitriding of titanium in low-energy electron beam excited plasma // Technical Physics Letters* Volume 35, Issue 8, 2009, Pages 713-716.
- [16] J.Sun, W.P.Tong, L.Zuo, Z.B.Wang *Low-temperature plasma nitriding of titanium layer on Ti/Al clad sheet // Materials & Design* Volume 47, 2013, Pages 408-415.
- [17] Akhmadeev, Yu.Kh., Goncharenko, I.M., Ivanov, Yu.F., Koval, N.N., Schanin, P.M. *Nitriding of technical-purity titanium in hollow-cathode glow discharge // Technical Physics Letters* Volume 31, Issue 7, 2005, Pages 548-550.
- [18] D. Batory, W. Szymanski, M. Panjan, O. Zabeida, J.E. Klemberg-Sapieha. *Plasma nitriding of Ti6Al4V alloy for improved water erosion resistance // Wear* 374-375 (2017) 120-127.
- [19] H. Michel, T. Czerwiec, M. Gantois, D. Ablitzer, A. Ricard. *Progress in the analysis of the mechanisms of ion nitriding // Surface and Coatings Technology* 72 (1995) 103-111.



- [20] T.M. Muraleedharan, E.I. Meletis. Surface modification of pure titanium and Ti-6Al-4V by intensified plasma ion nitriding // *Thin Solid Films* Volume 221, Issues 1–2, 10 December 1992, Pages 104-113.
- [21] K.C. Chen, G.J. Jaung. Dc diode ion nitriding behavior of titanium and Ti-6Al-4V // *Thin Solid Films* 303 (1997) 226-231.
- [22] Budilov, V.V., Agzamov, R.D., Ramazanov, K.N. Ion nitriding in glow discharge with hollow cathode effect // *Metal Science and Heat Treatment*. Volume 49, Issue 7-8, July 2007, Pages 358-361.
- [23] Ilyin, A.A., Skvortsova, S.V., Lukina, E.A., Karpov, V.N., Polyakov, O.A. Low-temperature ion nitriding of implants made of VT20 Ti alloy in different structural states // *Russian Metallurgy (Metally)* Volume 2005, Issue 2, March 2005, Pages 126-131.
- [24] F.D. Lai, T.I. Wu, J.K. Wu. Surface modification of Ti-6Al-4V alloy by salt cyaniding and nitriding // *Surface and Coatings Technology*. Volume 58, Issue 1, 18 June 1993, Pages 79-81.
- [25] Akio Nishimoto, Kimiaki Nagatsuka, Ryota Narita, Hiroaki Nii, Katsuya Akamatsu. Effect of the distance between screen and sample on active screen plasma nitriding properties // *Surface & Coatings Technology* 205 (2010) S365–S368.
- [26] L.N. Tang, M.F. Yan. Influence of Plasma Nitriding on the Microstructure, Wear, and Corrosion Properties of Quenched 30CrMnSiA Steel *Journal of Materials Engineering and Performance* July 2013, Volume 22, Issue 7, pp 2121–2129.
- [27] C. Zhao, C.X. Li, H. Dong, T. Bell. Study on the active screen plasma nitriding and its nitriding mechanism // *Surface and Coatings Technology* Volume 201, Issue 6, 4 December 2006, Pages 2320-2325.
- [28] Vershinin, D.S., Smolyakova, M.Y. Study of gas-mixture composition influence on structure and properties of titanium alloy VT6 at low-temperature nitriding // *Journal of Surface Investigation*. Volume 6, Issue 1, February 2012, Pages 159-164.
- [29] C. Muratore, D. Leonhardt, S.G. Walton, D.D. Blackwell, R.F. Fernsler, R.A. Meger. Low-temperature nitriding of stainless steel in an electron beam generated plasma // *Surface & Coatings Technology* 191 (2005) 255–262.
- [30] P. Abraha, Y. Yoshikawa, Y. Katayama. Surface modification of steel surfaces by electron beam excited plasma processing // *Vacuum* 83 (2009) 497–500.
- [31] Burdovitsin, V.A., Golosov, D.A., Oks, E.M., Tyunkov, A.V., Yushkov, Yu.G., Zolotukhin, D.B., Zavadsky, S.M. Electron beam nitriding of titanium in medium vacuum // *Surface and Coatings Technology*. Volume 358, 25 January 2019, Pages 726-731.
- [32] Gavrilov, N.V., Men'shakov, A.I. Effect of the electron beam and ion flux parameters on the rate of plasma nitriding of an austenitic stainless steel // *Technical Physics*. Volume 57, Issue 3, March 2012, Pages 399-404.
- [33] Burdovitsin, V.A., Oks, E.M. Fore-vacuum plasma-cathode electron sources // *Laser and Particle Beams* Volume 26, Issue 4, December 2008, Pages 619-635.
- [34] Korotaev, A.D. Multicomponent hard and superhard submicro- and nanocomposite coatings on the basis of titanium and iron nitrides / A.D. Korotaev, V.Yu. Moshkov, S.V. Ovchinnikov, Yu.P. Pinzhin, A.N. Tyumentsev, V.P. Sergeev, D.P. Borisov, V.M. Savostikov // *Physical Mesomechanics*. – 2007. – V. 10. – № 3–4. – P. 156–167.
- [35] N. Kashaev, H.-R. Stock, and P. Mayr. Nitriding of Ti-6% Al-4% V alloy in the plasma of an intensified glow discharge // *Metal Science and Heat Treatment*. Vol. 46, Nos. 7 – 8, 2004. P. 294 – 298.

**Declaration of interests**

The authors declare that they have no known competing financial interests or personal relationships that could have appeared to influence the work reported in this paper.

The authors declare the following financial interests/personal relationships which may be considered as potential competing interests:

Journal Pre-proof

Authors contributions

**Andrey Tyunkov:** Investigation, Writing – Original draft preparation. **Dmitry Golosov:** Conceptualization, Methodology. **Denis Zolotukhin:** Writing-Reviewing and Editing. **Alisa Nikonenko:** Investigation. **Efim Oks:** Supervision. **Yury Yushkov:** Investigation, Writing-Reviewing and Editing. **Yevgeny Yakovlev:** Investigation, Samples characterization.

Journal Pre-proof

Highlights

- E-beam used for sample heating and ions production enhances titanium nitriding
- Powerful e-beam and dense plasma are produced by a unique plasma electron source
- Beam sample heating increases efficiency and shortens nitriding time
- Such nitriding method improved sample microhardness and wear-resistance

Journal Pre-proof